Available online at www.sciencedirect.com
SCIENCE DIRECT®
International Journal of Heat and Mass Transfer 48 (2005) 3461–3468
International Journal of HEAT and MASS TRANSFER
www.elsevier.com/locate/ijhmt

Behavior of thermal plumes from two-heat sources in an enclosure

Koichi Ichimiya [a,*], Hideyuki Saiki [b]

[a] Mechanical Systems Engineering Division, Interdisciplinary Graduate School of Medicine and Engineering, University of Yamanashi, Takeda-4, Kofu, Yamanashi 400-8511, Japan
[b] Marusei Heavy Industry Co. Ltd., Naniwa-ku, Osaka-shi, Osaka 556-0021, Japan

Received 8 January 2004

Abstract

The present paper describes the upward motion, the interaction and the impingement heat transfer to the upper wall of two thermal plumes from two heated sections on a horizontal plate. Numerical analysis was performed for dimensionless pitch Pi = 0.26, 0.50, 0.76 and 1.0, Grashof number $Gr = 10^3$–10^6 and $Pr = 170$. Numerical results show that the upward motion is divided into three patterns depending on the pitch of two heated sections. The first pattern is the unification of two thermal plumes like one for short pitch. The second one is the separate upward motion after the unification. The third one is the independent motion for long pitch. These patterns were investigated by visualization of thermosensitive liquid crystal suspension. The impingement local heat transfer on the upper wall is evaluated transiently for various Grashof numbers. Mean Nusselt number depends on $Gr^{-0.16}$.

Keywords: Thermal engineering; Natural convection; Thermal plume; Two-heat sources; Numerical analysis; Thermosensitive liquid crystal suspension

1. Introduction

Thermal plumes are phenomena which we can find in cooling of an electric device, natural convective heat transfer in a comparatively small heat exchanger, a heat reservoir, an air conditioning in a room and also in an environmental problem such as a heat island or a warm water drainage. A thermal plume from one heat source or a line heat source has been extensively studied. Pera and Gebhart [1] investigated the hydrodynamic stability of a laminar plume arising from a horizontal line source of heat. Neutral stability curves were obtained in terms of the Grashof number. Noto [2] performed experimentally the sway spectrum, the sway frequency and several characteristics in the sway motion of a laminar thermal plume of air arising from a horizontal line source. Srinivasan and Angrirasa [3] presented a numerical study of laminar axisymmetric plumes that emanate from a source of combined buoyancy due to simultaneous heat and mass diffusion. Yang [4] studied the transition of a thermal plume from laminar to turbulent flow and proposed a new dispersion equation which accounts for the instability of all transverse modes on the plume. Hsu et al. [5] measured the temperature distribution of a developing thermal plume in an enclosure, generated by a constant heat flux annular cylinder heater and

* Corresponding author. Tel./fax: +81 55 220 84 34.
E-mail address: ichimiya@yamanashi.ac.jp (K. Ichimiya).

0017-9310/$ - see front matter © 2005 Elsevier Ltd. All rights reserved.
doi:10.1016/j.ijheatmasstransfer.2005.02.038

Nomenclature

a	thermal diffusivity of working fluid
b	width of heated section
B	dimensionless width = b/h
C	distance from the center to side wall
Cc	dimensionless heat flux constant on the upper wall
g	acceleration of gravity
Gr	Grashof number = $g\beta h^3(T_H - T_i)/v^2$
h	height of enclosure
H	dimensionless height = $h/h = 1$
Nu	local Nusselt number = $\alpha h/\lambda$
Nu_{mean}	average Nusselt number
Nu_{min}	minimum Nusselt number
P	pressure
pi	pitch of two-heat sources
Pi	dimensionless pitch of two-heat sources = pi/h
Pr	Prandtl number
q	heat flux
t	time
T	temperature
T_H	temperature of heat source
T_i	initial temperature
T_w	upper wall temperature
u	velocity along x direction
U	dimensionless velocity = uh/v
v	velocity along y direction
V	dimensionless velocity = vh/v
w	width of an enclosure
W	dimensionless width = w/h
x, y	coordinate system
X, Y	dimensionless coordinate system = x/h, y/h
α	heat transfer coefficient = $q/(T_w - T_i)$
β	expansion coefficient of working fluid
Θ	dimensionless temperature = $(T - T_i)/(T_H - T_i)$
λ	thermal conductivity of working fluid
v	kinetic viscosity of working fluid
τ	dimensionless time = tv/h^2
ϕ	stream function
Ψ	dimensionless stream function = ϕ/v
ω	vorticity
Ω	dimensionless vorticity = $\omega h^2/v$

evaluated the heat transfer. Fisher and Ball [6] measured the unsteady temperature fluctuations in the plume region between differentially heated horizontal concentric cylinders. Power spectrum density estimates of temperature fluctuation within the plume showed the development and breakdown of the oscillatory plume structure. Jiang and Luo [7] showed a spatial direct numerical simulation of an axisymmetric buoyant thermal plume. The fluid exhibits a periodic oscillatory motion known as the puffing phenomenon which is the formation and convection of vortex at the near field of the plume. Auban et al. [8] presented the experiment of a thermal plume in a confined stratified environment, a situation encountered in displacement ventilation systems. Criteria permitting definition of the interface elevation and thickness were determined based on statistical processing of concentration fluctuation. Degan et al. [9] investigated analytically about buoyancy induced convection arising from a horizontal line heat source embedded in an anisotropic porous medium. A minimum intensity of the thermal convective plume above the line source of heat can be obtained if the porous matrix is oriented with higher permeability parallel to the vertical direction. Ichimiya and Abe [10] presented a numerical calculation of the generation, growth and impingement of a thermal plume from a heated portion on the bottom of a rectangular enclosure. The local heat transfer on the upper wall was evaluated transiently for various spaces and Grashof numbers. Additionally, there are several researches on the wall plumes. Lai [11] studied weakly buoyant turbulent wall plumes for surface inclined 0–62° from the vertical. Low level of ambient stratification caused wall plumes to entrain fluid in the horizontal direction. Lin et al. [12] studied both theoretically and experimentally the inclined wall plumes which arise from a line thermal source embedded at the leading edge of an adiabatic plate with arbitrary tilt angle. Sangras et al. [13] described the measurements of the mixture fraction properties of plane buoyant turbulent adiabatic wall plumes, emphasizing conditions far from the source which self-preserving behavior is approximated. However, we practically can find several thermal plumes in heat generation from semi-conductors in electric device, the source of heat saving in heat accumulator, several buildings in a big city, and the phenomena change transiently. Thermal plumes from several heat sources behave in complicate form because of the interaction between thermal plumes and the unsteadiness. We focused on the thermal plumes from two-heat sources as a basic research of thermal plumes from plural heat sources. Gebhart et al. [14] observed the behavior of the flow unsteadiness and environmental effect using optical method for various intensities of thermal plumes. Brahimi et al. [15] studied a certain number of turbulent characteristics of the interacting flow of two thermal plumes of equal power, which contains the two separate regions. However, they have not yet studied the heat transfer characteristics.

In the present study, the basic behavior of two thermal plumes from two-heat sources on the bottom wall in an enclosure was examined using numerical calculation and flow visualization by thermosensitive liquid crystal suspension. We particularly paid attention to the rising patterns of thermal plumes and impingement heat transfer characteristics of the buoyancy induced jet to the upper wall.

2. Numerical analysis

Fig. 1 shows the two-dimensional coordinate system. The height, width of an enclosure and the width, pitch of two heated portions are h, w, b and pi, respectively. The distance from the center to side wall is C. The temperature of heated portions is T_H. The upper wall is heated slightly and uniformly to evaluate the impingement heat transfer of thermal plumes. Other walls are insulated thermally. The followings are assumed in the numerical analysis: (1) thermal properties are constant except for density, (2) Boussinesq approximation is applied in buoyancy induced term and (3) thermal radiation is neglected.

The pressure term in momentum equation was omitted by introducing stream function ϕ and vorticity ω. Governing equations were transformed into dimensionless form using dimensionless parameters in nomenclature. Dimensionless governing equations are as follows:

$$\frac{\partial^2 \Psi}{\partial X^2}+\frac{\partial^2 \Psi}{\partial Y^2}=-\Omega \tag{1}$$

$$\frac{\partial \Omega}{\partial \tau}+\frac{\partial \Psi}{\partial Y}\frac{\partial \Omega}{\partial X}-\frac{\partial \Psi}{\partial X}\frac{\partial \Omega}{\partial Y}=\left(\frac{\partial^2 \Omega}{\partial X^2}+\frac{\partial^2 \Omega}{\partial Y^2}\right)-Gr\frac{\partial \Theta}{\partial Y} \tag{2}$$

$$\frac{\partial \Theta}{\partial \tau}+\frac{\partial \Psi}{\partial Y}\frac{\partial \Theta}{\partial X}-\frac{\partial \Psi}{\partial X}\frac{\partial \Theta}{\partial Y}=\frac{1}{Pr}\left(\frac{\partial^2 \Theta}{\partial X^2}+\frac{\partial^2 \Theta}{\partial Y^2}\right) \tag{3}$$

Dimensionless initial condition is

at $\tau=0$: $\Psi=\Omega=\Theta=0$

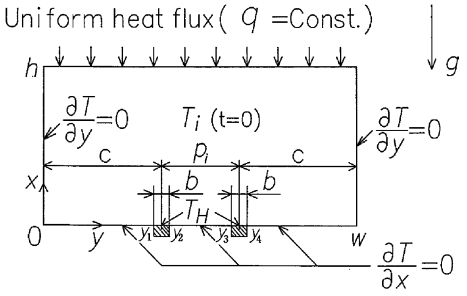

Fig. 1. Co-ordinate system.

Dimensionless boundary conditions are

at $\tau>0$,

$X=0,\ 0\leqslant Y\leqslant Y_1,\ Y_2\leqslant Y\leqslant Y_3,\ Y_4\leqslant Y\leqslant W$:

$\Psi=0,\ \partial\Theta/\partial X=0$

$X=0,\ Y_1\leqslant Y\leqslant Y_2,\ Y_3\leqslant Y\leqslant Y_4$: $\Psi=0,\ \Theta=1$

$0\leqslant X\leqslant 1,\ Y=0,\ Y=W$: $\Psi=0,\ \partial\Theta/\partial Y=0$

$X=1,\ 0\leqslant Y\leqslant W$: $\Psi=0,\ \partial\Theta/\partial X=\mathrm{Cc}[=qh/\lambda(T_H-T_i)]$

where Y_1, Y_2, Y_3 and Y_4 are the positions of the end of heating section. Cc is a dimensionless heat flux constant on upper wall to evaluate the impingement heat transfer of thermal plumes. In the present case, Cc is equal to 0.1003 corresponding to the flow visualization. Even if Cc changes, the upper wall temperature changes corresponding to Cc. Therefore, Cc does not affect intuitively the heat transfer on the upper wall.

The heat transfer on the upper wall was evaluated by local Nusselt number and average Nusselt number.

$$Nu=\alpha h/\lambda=\mathrm{Cc}/\Theta_{IE}$$

$$Nu_{mean}=(\mathrm{Cc}\cdot h/W)\int(1/\Theta_{IE})\,dY$$

where Θ_{IE} is dimensionless upper wall temperature.

The minimum size of dimensionless grids is 0.01 and the maximum total number of grids is 50 000. In numerical analysis, ADI method was applied for dimensionless temperature Θ and dimensionless vorticity Ω, and SOR method for dimensionless stream function Ψ. Conversion criteria is $|\Psi_{n+1}-\Psi_n|/|\Psi_{\max\ n+1}|\leqslant 5\times10^{-4}$, where n is iteration number. Numerical conditions are, dimensionless width of heated section B (=b/h) = 0.10, dimensionless height H (=h/h) = 1.0, dimensionless distance from the center to the side wall C (=c/h) = 0.75, dimensionless pitches of two heated sections Pi = 0.26, 0.50, 0.76 and 1.0, dimensionless aspect ratios H/W = 0.568, 0.5, 0.442 and 0.40, Grashof number $Gr=10^3$–10^6 and Prandtl number Pr = 170 corresponding to silicone oil in flow visualization.

3. Visualization by thermosensitive liquid crystal suspension

The size of an enclosure is 100 mm high and 200 mm wide, and two heated sections (10 mm wide each) are set at 75 mm from both sides. The upper wall is composed of a thermosensitive liquid crystal sheet, a stainless steel foil (20 μm thick) and a bounding sheet with more than 90% transparency on a transparent acrylic plate (10 mm thick). The thermosensitive liquid crystal particles with 50 μm diameter were mixed with silicone oil at the rate 0.2% weight to visualize the temperature change corresponding to the color change and the flow with the behavior of particles. The allowable temperature range

is from 24 to 28 °C for liquid crystal suspension and from 24 to 29 °C for liquid crystal sheet.

4. Results and discussions

The behavior of two thermal plumes are presented by dimensionless temperature Θ and dimensionless stream function Ψ in Figs. 2 and 3 for Pi = 0.50 and $Gr = 10^4$. The inclined lines on abscissa are two heated sections. The buoyancy induced two thermal plumes rise up separately over the critical Reynolds number based on the thickness of thermal conduction layer and develop like mushrooms. On the upper wall, a thermal conductive layer is generated due to a uniform heat flux (Fig. 2(a)). At $\tau = 4.5 \times 10^{-1}$ (Fig. 2(b)), high temperature portions for $\Theta = 0.3$ and 0.6 go up with approaching each other and moving to inner side, and isothermal line $\Theta = 10^{-4}$ envelopes both thermal plumes. At the top of the plume a closed high temperature portion $\Theta = 0.1$ is produced. Between two thermal plumes, the flow is accelerated and the pressure reduces. Additionally, a recirculating flow is generated between the center of the vessel and the side wall. That is why two thermal plumes move to the center. In the next stage, the separate high temperature portions impinge to the upper wall through a thermal conduction layer. At $\tau = 7.2 \times 10^{-1}$ (Fig. 2(c)), comparatively high temperature layer $\Theta = 0.1$ and 0.3 moves up and low temperature layers $\Theta = 10^{-3}$ and 10^{-2} go downward from the upper wall. At $\tau = 9.0 \times 10^{-1}$ (Fig. 2(d)), the isothermal line $\Theta = 0.1$ rises up and pushes low temperature layer. Corresponding to the temperature field, two small recirculating flows are generated near the heating sections according to dimensionless stream function, and two large symmetric recirculating flows are produced between two side walls and two rising flows (Fig. 3(a)). At $\tau = 4.5 \times 10^{-1}$, two recirculating flows grow up with curving and the centers move up to $X = 0.6$ (Fig. 3(b)). After two plumes impinge the upper wall, two centers of recirculating flows fall down and two recirculating flows are kept near the heated section (Fig. 3(c) and (d)). The curves of two thermal plumes were visualized using thermosensitive liquid suspension (Fig. 4(a)). The rising velocity of the plumes is from several mm/s to 10 mm/s. The extension of the top of plumes after the unification and the thermal stratification near the upper wall agree qualitatively with the numerical results (Fig. 4(b)).

Fig. 5(a) and (b) shows the dimensionless temperature Θ and the dimensionless stream function Ψ in the narrower space (Pi = 0.26, $Gr = 10^4$ and $\tau = 4.5 \times 10^{-1}$). High temperature isothermal lines $\Theta = 0.3$ from two heated portions combine due to narrow space and it behaves as if it is a single thermal plume. Therefore, the dimensionless stream function produces two large recirculating flows. In wider pitch (Pi = 1.0, $Gr = 10^4$ and $\tau = 4.5 \times 10^{-1}$), as Fig. 6(a) and (b) presents, two thermal plumes rise independently without interaction until they impinge the upper wall, and they generate the thermal stratification near the upper wall. As the result, four recirculating flows are generated and the centers move up to the upper wall. The gradient of Ψ along Y direction is high at the boundary of a small

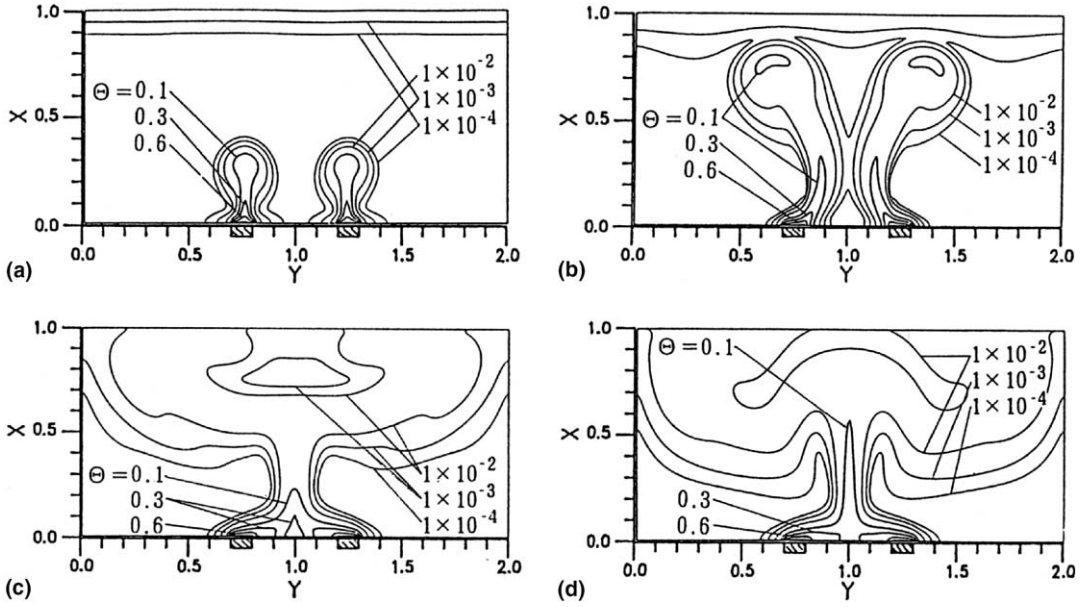

Fig. 2. Isothermal lines (Pi = 0.5, $Gr = 10^4$): (a) $\tau = 2.7 \times 10^{-1}$, (b) $\tau = 4.5 \times 10^{-1}$, (c) $\tau = 7.2 \times 10^{-1}$ and (d) $\tau = 9 \times 10^{-1}$.

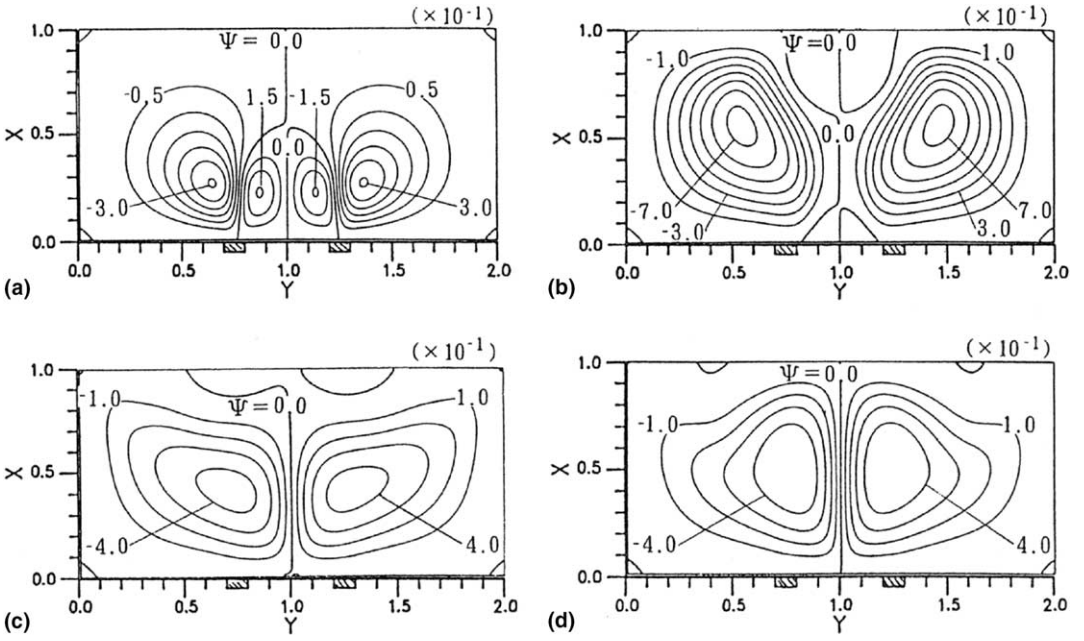

Fig. 3. Dimensionless stream function (Pi = 0.5, $Gr = 10^4$): (a) $\tau = 2.7 \times 10^{-1}$, (b) $\tau = 4.5 \times 10^{-1}$, (c) $\tau = 7.2 \times 10^{-1}$ and (d) $\tau = 9 \times 10^{-1}$.

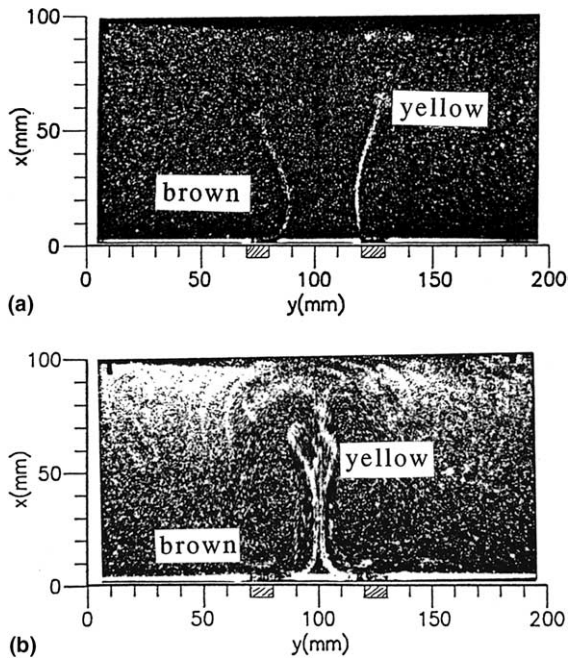

Fig. 4. Color distribution of two thermal plumes (Pi = 0.5, $Gr = 4 \times 10^4$): (a) two separate thermal plumes ($\tau = 4.5 \times 10^{-2}$) and (b) unification of two thermal plumes ($\tau = 1.3 \times 10^{-1}$).

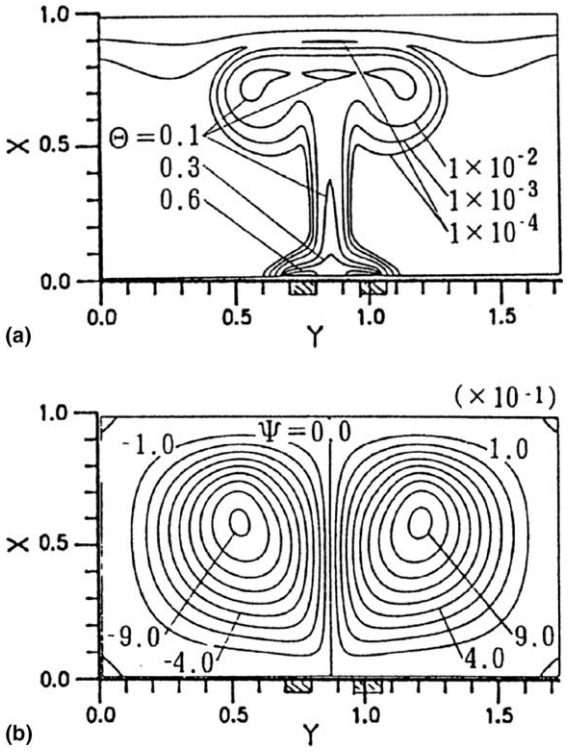

Fig. 5. Isothermal lines and dimensionless stream function (Pi = 0.26, $Gr = 10^4$, $\tau = 4.5 \times 10^{-1}$): (a) isothermal lines and (b) dimensionless stream function.

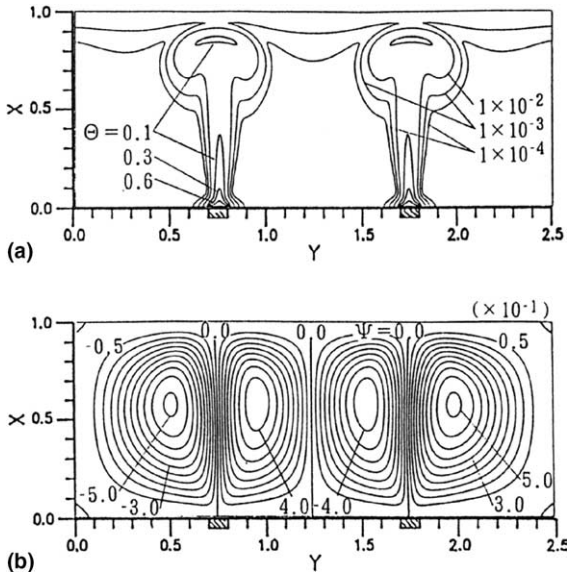

Fig. 6. Isothermal lines and dimensionless stream function (Pi = 1.0, $Gr = 10^4$, $\tau = 4.5 \times 10^{-1}$): (a) isothermal lines and (b) dimensionless stream function.

recirculating flow and a large one. This means the velocity along X direction is large.

The flow pattern depends on the pitch of two heated portions until two thermal plumes approach to the upper wall and is divided into three, namely, (1) two thermal plumes combine each other and move up as if they are a single plume, (2) after two thermal plumes combine, they separate again as they move up, and (3) two thermal plumes move up independently without interaction. In the final stage, these aspects are estimated to become weak with the reduction of the temperature difference between the heated section and the fluid. The situation in the final stage will be discussed in detail for various conditions in the next chance.

Fig. 7(a)–(c) shows the local Nusselt number, Nu as a parameter of time τ corresponding to the temperature and flow field described above. In Fig. 7(a) (Pi = 0.26), two thermal plumes move up like a single thermal plume, and after they impinge the upper wall, they separate to both sides. Therefore, the local Nusselt number takes three minimum values at $\tau = 7.2 \times 10^{-1}$. The positions of two minimum values at both ends move to side walls with time. In Fig. 7(b) (Pi = 0.50), as bifurcated

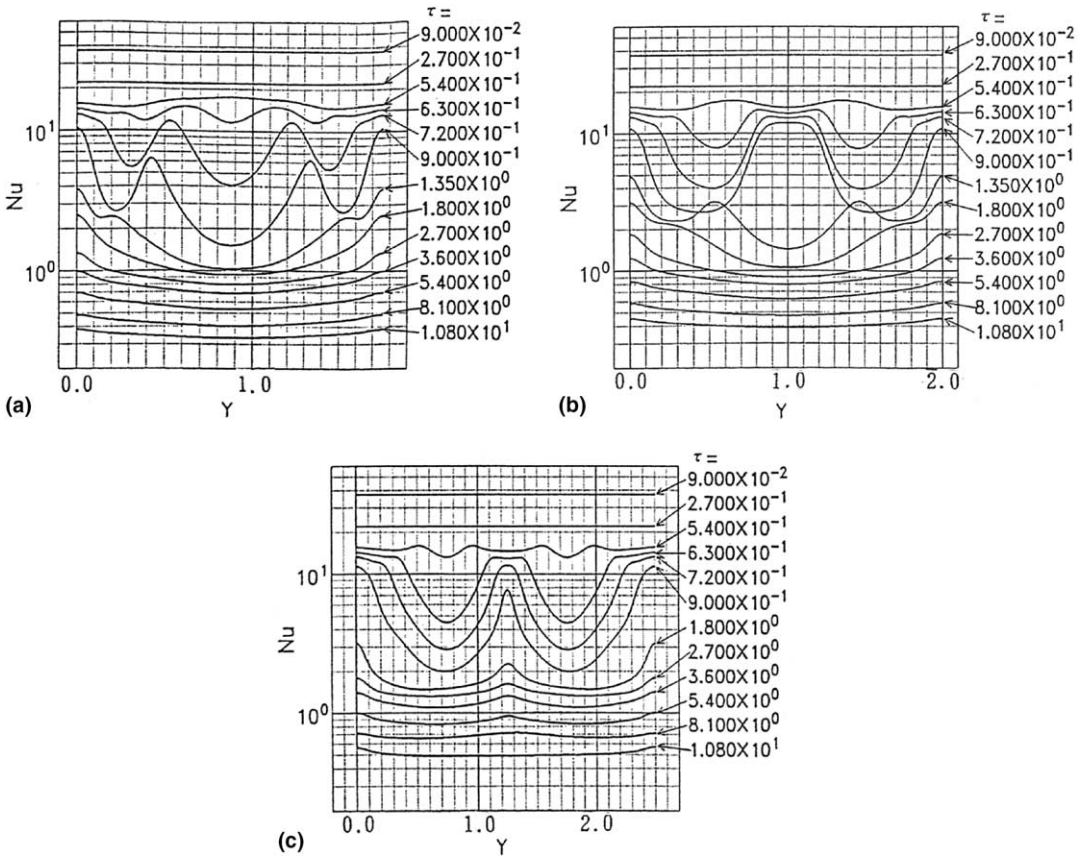

Fig. 7. Local Nusselt number ($Gr = 10^4$): (a) Pi = 0.26, (b) Pi = 0.50 and (c) Pi = 1.0.

plumes impinge the upper wall, the local Nusselt number takes two minimum value at the boundary of the center. At $\tau = 1.8$, it is minimal at the center because a high temperature plume follows and impinges. In Fig. 7(c) (Pi = 1.0), two thermal plumes impinge independently the upper wall and take two minimums. The position of the minimum value does not change transiently. The local Nusselt number behaves uniformly along width after $\tau = 5.4$ due to the temperature increase in the vessel. It means that the effect of the local behavior of thermal plumes is weakened with the generation of the thermal stratification near the upper wall.

The heat transfer on the wall depends on the impingement of the buoyancy induced flow. In order to examine the effect of Grashof number, Fig. 8 shows the local Nusselt number for a high Grashof number $Gr = 10^5$. The local Nusselt number behaves slightly like a wave because the temperature difference between the heated portion and the fluid is high, and a high temperature portion in a plume impinges the upper wall. In $Gr = 10^6$, plumes behave unstably and asymmetrically.

In the next step, the local Nusselt number was averaged along the upper wall. Fig. 9 shows the transient mean Nusselt number as a parameter of Gr. The mean Nusselt number Nu_{mean} changes in two steps at $\tau = 2.5$ for $Gr = 10^3$ and $\tau = 0.5$ for $Gr = 10^4$. After $\tau = 5$, Nu_{mean} has the constant gradient $dNu_{mean}/d\tau$ for four Grashof numbers. Dimensionless time $\tau = 5$ means the time region that the behavior of the local Nusselt number becomes flat.

According to Fig. 9, Nu_{mean} has the stable region after $\tau = 5$ for various Gr numbers. The relationship between Gr and Nu_{mean} at $\tau = 10$, which the behavior of the local Nusselt number is stable, is representatively presented in Fig. 10 to examine the dependence of Nu_{mean} on Gr. The relation is expressed as $Nu_{mean} \sim Gr^{-0.16}$. The index of Gr is -0.16 and the absolute value

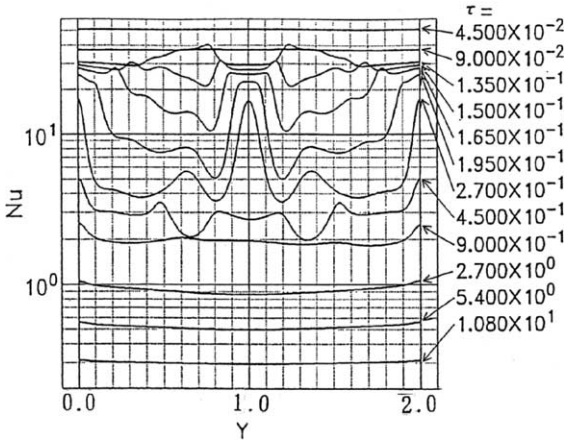

Fig. 8. Local Nusselt number (Pi = 0.5, $Gr = 10^5$).

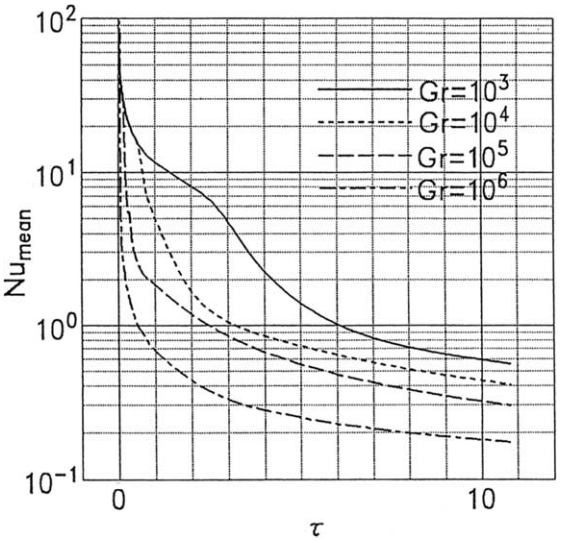

Fig. 9. Transient mean Nusselt number (Pi = 0.5).

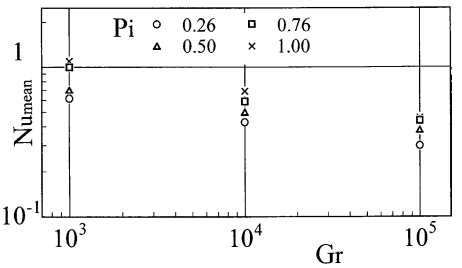

Fig. 10. Mean Nusselt number.

is less than the index of Gr on a single plume -0.2 [10]. This expresses that the interaction of two thermal plumes reduces the effect of Gr on the heat transfer to the upper wall.

5. Conclusions

The behavior of two thermal plumes from two heated portions on the bottom of an enclosure was analyzed numerically and was compared with visualization. Additionally, the heat transfer characteristics on the upper wall by impingement of thermal plumes were also evaluated. The flow patterns of thermal plumes from the bottom to the upper wall are divided into three due to the pitch of two heated portions, namely, (1) two thermal plumes combine each other and move up as if they are a single plume, (2) after two thermal plumes combine each other, they separate again with an ascent, and (3) two thermal plumes rise up independently without interaction. The local Nusselt number takes minimum values corresponding to these flow patterns, The position and

number of minimum values change with time. The mean Nusselt number, Nu_{mean}, depends on $Gr^{-0.16}$. The absolute value of the index of Gr is less than that of a single thermal plume, -0.2.

References

[1] L. Pera, B. Gebhart, On the stability of laminar plumes: some numerical solutions and experiments, Int. J. Heat Mass Transfer 14 (1971) 975–984.

[2] K. Noto, Swaying motion in thermal plume above a horizontal line heat source, J. Thermophys. Heat Transfer 3–4 (1989) 428–434.

[3] J. Srinivasan, D. Angrirasa, Laminar axisymmetric multicomponent buoyant plumes in a thermally stratified medium, Int. J. Heat Mass Transfer 33 (1990) 1751–1757.

[4] H.Q. Yang, Buckling of a thermal plume, Int. J. Heat Mass Transfer 35 (1992) 1527–1532;
H.Q. Yang, Int. J. Heat Mass Transfer. 14 (1971) 975–984.

[5] C.H. Hsu, C.F. Hsieh, J.T. Teng, Temperature measurement of a transient thermal plume in a confined space, J. Heat Transfer (TN) 119 (1997) 389–391.

[6] C.E. Fisher, K.S. Ball, Plume dynamics in natural convection in a horizontal cylindrical annulus, Trans. ASME, Ser. C 121 (1999) 598–602.

[7] X. Jiang, K.H. Luo, Direct simulation of the puffing phenomenon of an axisymmetric thermal plume, Theoret. Comput. Fluid Dyn. 14 (2000) 55–74.

[8] O. Auban, F. Lemoine, P. Vallette, J.R. Fontaine, Simulation by slutal convection of a thermal plume in a confined stratified environment: application to displacement ventilation, Int. J. Heat Mass Transfer 44 (2001) 4679–4691.

[9] G. Degan, S. Zohoun, P. Vasseur, Buoyant plume above a line source of heat in an anisotropic porous medium, Heat Mass Transfer 39 (2003) 209–213.

[10] K. Ichimiya, T. Abe, Impingement heat transfer of a single thermal plume on the upper wall, Int. J. Heat Mass Transfer 46 (2003) 3521–3528.

[11] M.C. Lai, Structure of turbulent adiabatic wall plumes, J. Heat Transfer 108 (1986) 827–834.

[12] H.T. Lin, J.J. Chen, L.W. Kung, W.S. Yu, Y.M. Chen, Inclined and horizontal wall plumes, Int. J. Heat Mass Transfer 39 (1996) 2243–2252.

[13] R. Sangras, Z. Dai, G.M. Faeth, Mixture fraction statistics of plane self-preserving buoyant turbulent adiabatic wall plumes, Trans. ASME, Ser. C 121 (1999) 837–843.

[14] B. Gebhart, H. Shaukatullah, L. Pera, The interaction of unequal laminar plane plumes, Int. J. Heat Mass Transfer 19 (1976) 751–756.

[15] M. Brahimi, L. Dehmani, D.K. Son, Turbulent structure of the interacting flow of two thermal plumes, Int. J. Heat Mass Transfer 32 (1989) 1551–1559.